

The Role of Interaction in the Pairing of Two Spin-orbit Coupled Fermions

Chong Ye,^{1,2} Jie Liu,^{1,3} Li-Bin Fu^{1,3,*}

¹National Laboratory of Science and Technology on Computational Physics,
Institute of Applied Physics and Computational Mathematics, Beijing 100088, China

²Graduate School, China Academy of Engineering Physics, Beijing 100088, China

³HEDPS, Center for Applied Physics and Technology, Peking University, Beijing 100084, China

We investigate the role of a repulsive s-wave interaction in the two-body problem in the presence of spin orbit couplings, motivated by current interests in exploring exotic superfluid phases in spin-orbit coupled Fermi gases. For weak spin orbit coupling where the density of states is not significantly altered, we analytically show that the high-energy states become more important in determining the binding energy when the interaction strength decreases. Consequently, tuning the interaction gives rise to a rich ground state behavior, including a zigzag of the ground state momentum or inducing transitions among the meta-stable states. By exactly solving the two-body problem for a spin-orbit coupled Fermi mixture of ^{40}K - ^{40}K - ^6Li , we demonstrate that our analysis can also apply to the case when the density of states is significantly modified by the spin-orbit coupling. Our findings pave the way for understanding and controlling the pairing of fermions in the presence of spin orbit couplings.

PACS numbers: 67.85.Hj, 03.65.Vf, 05.30.Rt

Introduction. Exploring the exotic superfluid phases [1–15] has become a major focus of research in ultracold Fermi gases, driven in particular by the realization of synthetic spin orbit couplings (SOC) [16–19]. At the core of these superfluid phenomena is the pairing of fermions, which can be understood from the perspective of two-body quantum mechanics [20–30]. The two-body problem in general contains three components: the threshold energy associated with the center-of-mass (c.m.) momentum, the density of states that contribute to the pairing, and the interacting strength. The former two can be significantly altered by SOC, which has been considered as the origin of the variety of exotic behavior of two binding fermions reported recently [23, 24, 26, 28]. However, the mechanism as to how all these three components cooperate with each other in determining the novel two-body properties remains unexplored. The establishment of such a comprehensive picture will shed light on ongoing explorations of the intriguing behavior of spin-orbit coupled Fermi gases [23–30]. Below, we report a theoretical contribution to address this issue, which also allows predictions of new phenomena.

We investigate the pairing of two spin-orbit coupled fermions in the presence of a repulsive s-wave interaction, the strength of which can be tuned in a wide range. By decomposing the two-body energy into the threshold energy and the binding energy, both of which depend on the c.m. momentum of the fermionic pair, we establish a direct relation between the interaction, the density of states, and the binding energy. In the limit of weak SOC, our first-order perturbation analysis reveal that the low energy states play decisive role in determining the binding energy when the interaction is strong, in contrast to the weak interaction case where high energy states can dominate. This allows us to elucidate the mechanism underlying interesting phenomena such as a zigzag

behavior of the ground state momentum and the competition between two meta-stable states. We illustrate our analysis for an interacting Fermi mixtures of ^{40}K - ^{40}K - ^6Li with ^{40}K which contains an equal weight combination of Rashba-type and Dresselhaus-type SOC, which can be realized by the state of the art experimental techniques using cold atoms [19, 32]. Remarkably, by exactly solving the two-body problem for this system, we show that our analysis afford insight into the main properties of the pairing of spin-orbit coupled fermions, even when the density of states is significantly altered by SOC. Our findings reveal the role of interaction in the pairing of two spin-orbit coupled fermions and allow deep physical understandings of the rich pairing physics in the presence of SOC.

Two-body binding with SOC. We consider a three dimensional (3D) Fermi-Fermi mixture consisting of two different fermionic atoms: atom A (B) has a SOC of N_a (N_b) components, with the corresponding non-interacting Fermi gas described by Hamiltonian H_a (H_b). We assume a repulsive s-wave contact interaction between the two fermionic species as described by $H_{\text{int}} = \frac{U}{V} \sum_{\mathbf{k}, \mathbf{k}', \mathbf{Q}} a_{\mathbf{k}, l_0}^\dagger b_{\mathbf{Q}-\mathbf{k}, m_0}^\dagger a_{\mathbf{k}', l_0} b_{\mathbf{Q}-\mathbf{k}', m_0}$, with \mathbf{Q} the c.m. momentum of two scattering fermions. Here $a_{\mathbf{k}, l_0}^\dagger$ ($b_{\mathbf{k}, m_0}^\dagger$) denotes the creation operator of a SOC-free atom A (B) in l_0 (m_0) spin component with momentum \mathbf{k} , U is the bare interaction, and V is the volume. The total Hamiltonian for the interacting Fermi-Fermi mixture is thus $H = H_a + H_b + H_{\text{int}}$.

To study the two-body quantum mechanics for binding two fermionic atoms A and B on top of a Fermi sea denoted by $|FS\rangle$, we use the energy eigenbasis of Hamiltonians H_a and H_b , where we adopt an ansatz for the two-body wave function $|\Psi_{\mathbf{Q}}\rangle = \sum_{i,j} \sum_{\mathbf{k}} \psi_{\mathbf{Q}, \mathbf{k}}^{i,j} \alpha_{\mathbf{k}, i}^\dagger \beta_{\mathbf{Q}-\mathbf{k}, j}^\dagger |FS\rangle$, which describes creation of fermionic pairs with a c.m. momentum \mathbf{Q} . Here,

$\alpha_{\mathbf{k},i}^\dagger$ ($\beta_{\mathbf{k},i}^\dagger$) is the creation operator of a spin-orbit coupled atom A (B) in i "helicity" with momentum \mathbf{k} and $\psi_{\mathbf{Q},\mathbf{k}}^{i,j}$ denotes the variational coefficient. Moreover, the summation $\sum_{\mathbf{k}}$ excludes the states below the Fermi surface, reflecting the effect of Pauli blocking. Solving the eigen-equation $H|\Psi_{\mathbf{Q}}\rangle = E_{\mathbf{Q}}|\Psi_{\mathbf{Q}}\rangle$ gives

$$\psi_{\mathbf{Q},\mathbf{k}}^{i,j} = \frac{(\lambda_{\mathbf{k}}^{i,l_0} \eta_{\mathbf{Q}-\mathbf{k}}^{j,m_0})^*}{E_{\mathbf{Q}} - E_{\mathbf{Q},\mathbf{k}}^{ij}} \frac{U}{V} \sum_{\mathbf{k}',i',j'}' \psi_{\mathbf{Q},\mathbf{k}'}^{i',j'} \lambda_{\mathbf{k}'}^{i',l_0} \eta_{\mathbf{Q}-\mathbf{k}'}^{j',m_0}, \quad (1)$$

with $E_{\mathbf{Q},\mathbf{k}}^{ij} = \varepsilon_{\mathbf{k},i}^a + \varepsilon_{\mathbf{Q}-\mathbf{k},j}^b$, $\lambda_{\mathbf{k}}^{i,l_0} = \langle FS | a_{\mathbf{k},l_0} \alpha_{\mathbf{k},i}^\dagger | FS \rangle$ and $\eta_{\mathbf{Q}-\mathbf{k}}^{j,m_0} = \langle FS | b_{\mathbf{Q}-\mathbf{k},m_0} \beta_{\mathbf{Q}-\mathbf{k},j}^\dagger | FS \rangle$. Rearranging Eq. (1), we obtain a self-consistent equation for $E_{\mathbf{Q}}$ in the momentum-space representation, i.e.,

$$\frac{1}{U} = \frac{1}{V} \sum_{i,j} \sum_{\mathbf{k}}' \frac{|\lambda_{\mathbf{k}}^{i,l_0}|^2 |\eta_{\mathbf{Q}-\mathbf{k}}^{j,m_0}|^2}{E_{\mathbf{Q}} - E_{\mathbf{Q},\mathbf{k}}^{ij}}. \quad (2)$$

A key step of our treatment next constitutes a decomposition of $E_{\mathbf{Q}}$: Defining the threshold energy involving only the c.m. momentum \mathbf{Q} by $E_{\text{th}}^{\mathbf{Q}} \equiv \min_{\mathbf{k}} \{E_{\mathbf{Q},\mathbf{k}}^{ij}\}$, we write $E_{\mathbf{Q}}^{ij} = E_{\text{th}}^{\mathbf{Q}} + \varepsilon$. The rest of the two-body energy is therefore $E_{\mathbf{Q}}^{sc} \equiv E_{\mathbf{Q}} - E_{\text{th}}^{\mathbf{Q}}$. While $E_{\text{th}}^{\mathbf{Q}}$ is only affected by SOC, $E_{\mathbf{Q}}^{sc}$ encodes the effect of interaction. Such decomposition of $E_{\mathbf{Q}}$ in terms of $E_{\mathbf{Q}}^{sc}$ and $E_{\text{th}}^{\mathbf{Q}}$, as we shall see, allows a transparent correspondence to the SOC-free counterpart. Transforming Eq. (2) into an integral in the energy domain of ε via standard procedures, we obtain

$$\int_0^\infty \frac{\gamma_{\mathbf{Q}}^\varepsilon d\varepsilon}{E_{\mathbf{Q}}^{sc} - \varepsilon} = \frac{1}{U}. \quad (3)$$

Here, $\gamma_{\mathbf{Q}}^\varepsilon$ is defined by

$$\gamma_{\mathbf{Q}}^\varepsilon = \sum_i \sum_j \int' |\lambda_{\mathbf{k}}^{i,l_0}|^2 |\eta_{\mathbf{Q}-\mathbf{k}}^{j,m_0}|^2 |J| d\nu d\mu, \quad (4)$$

which describes the density of states contributing to the pairing in 3D (states below the Fermi surface have been excluded from integration)[33]. In Eq. (4), μ and ν label the degrees of freedom other than ε , and J denotes the standard Jacobian. For fixed \mathbf{Q} , $\gamma_{\mathbf{Q}}^\varepsilon$ is determined by SOC and the spin-orbit coupled Fermi energy. Note that above formulas can be easily adapted to describe the pairing of fermions in the vacuum.

Equation (3) establishes a direct relation between the interaction U , the density of states $\gamma_{\mathbf{Q}}^\varepsilon$, and $E_{\mathbf{Q}}^{sc}$. Intuition behind it can be gained in the limit of vanishing SOC, where $E_{\text{th}}^{\mathbf{Q}} = \mathbf{Q}^2/(2m_\mu)$ with m_μ the reduced mass of the fermion pair, and $\gamma_{\mathbf{Q}}^\varepsilon = \gamma_0^\varepsilon = 2\sqrt{2m_\mu\varepsilon}$. Then, $E_{\mathbf{Q}}^{sc}$ is independent of \mathbf{Q} as ensured by Eq. (3), and can be identified as $E_{\mathbf{Q}}^{sc} \equiv \varepsilon_b = -1/(2m_\mu a_s^2)$ [$\hbar \equiv 1$] with $a_s > 0$ the s-wave scattering length, i.e., the binding energy of a molecule at rest. In this case, Eq. (3) reduces to,

in the momentum space representation, the well known renormalization equation for two scattering particles, i.e., $1/U = m_\mu/(2\pi a_s) - (1/V) \sum_{\mathbf{k}} (2m_\mu/\mathbf{k}^2)$. Equation (3) thus extends the standard prescription for two interacting fermions to the presence of SOC, where $E_{\mathbf{Q}}^{sc}$ is the counterpart of the molecular binding energy ε_b .

The role of interaction. Based on above treatment, below we elucidate how the interaction interplays with the effect of SOC in determining the behavior of $E_{\mathbf{Q}}^{sc}$, when the interaction strength U is tuned in a wide range via Feshbach resonance [31]. To compare to the SOC-free case, we introduce the quantity $\xi_{\mathbf{Q}} \equiv E_{\mathbf{Q}}^{sc} - \varepsilon_b$. For weak SOC that does not significantly alter the density of states, the leading term of $\xi_{\mathbf{Q}}$ can be derived from Eq. (3) as [34]:

$$\xi_{\mathbf{Q}} = - \left[\int_0^\infty \frac{\gamma_{\mathbf{Q}}^\varepsilon}{(\varepsilon - \varepsilon_b)^2} d\varepsilon \right]^{-1} \int_0^\infty \frac{\gamma_{\mathbf{Q}}^\varepsilon - \gamma_0^\varepsilon}{\varepsilon - \varepsilon_b} d\varepsilon. \quad (5)$$

Here we have ignored the modification of the renormalization relation by SOC [35–39]. In discussing the effect of interaction on $\xi_{\mathbf{Q}}$, we will be interested in (i) $\frac{\partial \xi_{\mathbf{Q}}}{\partial a_s^{-1}}$ and (ii) $\Delta_{\mathbf{Q}\mathbf{Q}'} \equiv \xi_{\mathbf{Q}'} - \xi_{\mathbf{Q}}$: The sign of the former reflects how $\xi_{\mathbf{Q}}$ for fixed \mathbf{Q} changes with interaction, while that of the latter tells whether a large or small \mathbf{Q} is energetically favored for a given interaction. Using Eq. (5), we find $\frac{\partial \xi_{\mathbf{Q}}}{\partial a_s^{-1}} \propto \int_0^\infty (\gamma_{\mathbf{Q}}^\varepsilon - \gamma_0^\varepsilon) d\varepsilon$ [40], and $\Delta_{\mathbf{Q}\mathbf{Q}'} \simeq - \left[\int_0^\infty \frac{\gamma_{\mathbf{Q}}^\varepsilon}{(\varepsilon - \varepsilon_b)^2} d\varepsilon \right]^{-1} \int_0^\infty \frac{\gamma_{\mathbf{Q}'}^\varepsilon - \gamma_{\mathbf{Q}}^\varepsilon}{\varepsilon - \varepsilon_b} d\varepsilon$, both relying crucially on $\gamma_{\mathbf{Q}}^\varepsilon$ [see Eq. (4)]. Thus, while the form of $\gamma_{\mathbf{Q}}^\varepsilon$ varies with specific setups, its qualitative analysis affords insight into generic behavior of $\xi_{\mathbf{Q}}$, as we elaborate next.

Consider first the simplest case where $\gamma_{\mathbf{Q}}^\varepsilon - \gamma_0^\varepsilon > 0$ for all energy levels ε [41], i.e., SOC induces an increase in the number of available scattering states at all energies. From Eq. (5), we see $\xi_{\mathbf{Q}} < 0$, hence pairing with finite \mathbf{Q} leads to an energy decrease as compared to the SOC-free case, irrespective of the interacting strength. Such energy drop, following from $\frac{\partial \xi_{\mathbf{Q}}}{\partial a_s^{-1}} > 0$, can be further enhanced by increasing a_s^{-1} . If, moreover, $\gamma_{\mathbf{Q}}^\varepsilon$ increases monotonically with \mathbf{Q} , we have $\Delta_{\mathbf{Q}\mathbf{Q}'} < 0$, i.e., $\xi_{\mathbf{Q}}$ decreases with increasing \mathbf{Q} for fixed scattering length. The amplitude of this decrease can be controlled by tuning the scattering length, which enhances with increased a_s^{-1} .

In contrast, if the effect of SOC is such that $\gamma_{\mathbf{Q}}^\varepsilon - \gamma_0^\varepsilon$ alters sign depending on the energy ε of the state, $\xi_{\mathbf{Q}}$ can exhibit a very rich behavior. To demonstrate it, consider $\gamma_{\mathbf{Q}}^\varepsilon - \gamma_0^\varepsilon$ has opposite sign in the low- and high-energy regimes, with a sign flip occurring at the energy ε_0 . Applying the mean value theorem to Eq. (5), we find $\int_0^\infty \frac{\gamma_{\mathbf{Q}}^\varepsilon - \gamma_0^\varepsilon}{\varepsilon - \varepsilon_b} d\varepsilon = f_l/(\varepsilon_1 - \varepsilon_b) + f_h/(\varepsilon_2 - \varepsilon_b)$, with $\varepsilon_1 \in (0, \varepsilon_0)$, and $\varepsilon_2 \in (\varepsilon_0, \infty)$. Here $f_l = \int_0^{\varepsilon_0} (\gamma_{\mathbf{Q}}^\varepsilon - \gamma_0^\varepsilon) d\varepsilon$ and $f_h = \int_{\varepsilon_0}^\infty (\gamma_{\mathbf{Q}}^\varepsilon - \gamma_0^\varepsilon) d\varepsilon$ are the number of scattering states in the low and high energy regimes, respectively. Since f_l and f_h have opposite signs, the contribution from the high energy states to $\xi_{\mathbf{Q}}$ is suppressed by the smaller

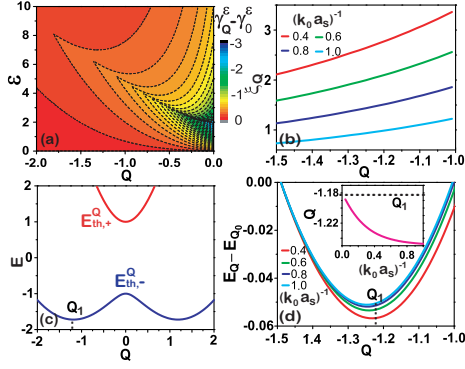


Figure 1. Pairing of fermions with SOC in a vacuum. (a) The distribution of $\gamma_Q^\epsilon - \gamma_0^\epsilon$. (b) ξ_Q as a function of Q with different $(k_0 a_s)^{-1}$ according to Eq.(5). (c) The threshold energy $E_{th}^Q = \min\{E_{th,-}^Q, E_{th,+}^Q\}$. $E_{th,+}^Q$ ($E_{th,-}^Q$) is the threshold energy of a particle A in the upper (lower) helicity branch and a particle B with a c.m. momentum Q . (d) The two-body energy with different interacting strengths by exactly solving Eq. (2). The inset shows the variation of the ground state c.m. momentum. Here $Q_0 = -1.5k_0 e_x$.

pre-factor compared to the low energy states. Yet, such suppression becomes less significant when a_s^{-1} increases, following similar reasoning as before. We thus expect the sign of ξ_Q to be mainly determined by the low energy states for large a_s , whereas high energy states can become decisive for small a_s . This has interesting physical implications: by tuning the scattering length and hence the sign of ξ_Q and $\Delta Q Q$, we can control whether a bound pair favors nonzero Q , and even the specific choice of Q .

Typical behaviors of ground states. We now show that, combining E_{th}^Q , above insight into the combined effects of interaction and SOC on E_Q^{sc} allows predictions on generic features of the dispersion E_Q . This can be best illustrated in two following cases.

(i) If E_{th}^Q has only one minimum, without interaction, the ground state c.m. momentum Q_g will locate at Q_1 where E_{th}^Q is minimized. By contrast, adding interaction can strongly modify E_Q^{sc} and thus E_Q , according to previous analysis, which renders Q_g to deviate from Q_1 . How far is such deviation intimately depends on the behavior of E_Q^{sc} : If E_Q^{sc} varies monotonically with Q for fixed scattering length, Q_g shifts from Q_1 in such a way that a smaller E_Q^{sc} can be reached. Such shift can be further enhanced by increasing a_s^{-1} , provided it does not qualitatively alter the behavior of E_Q^{sc} , i.e., E_Q^{sc} stays increasing (or decreasing) with Q when varying a_s^{-1} [c.f. inset of Fig. 1(d)]. If, instead, the behavior of E_Q^{sc} undergoes a qualitative change when a_s^{-1} increases, e.g. from increasing to decreasing with Q [see inset of Fig. 2(c)], Q_g will first exhibit a zigzag away from Q_1 before increasing above Q_1 monotonically [see inset of Fig. 2(d)].

(ii) In general E_{th}^Q can have multiple local minima, each corresponding to a meta-stable state. For individ-

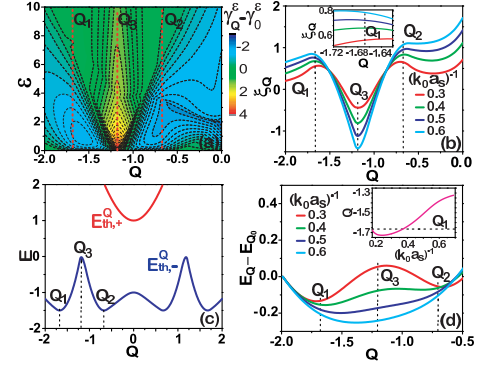


Figure 2. Pairing of Fermions with SOC on top of a Fermi sea. (a) The distribution of $\gamma_Q^\epsilon - \gamma_0^\epsilon$. (b) ξ_Q as a function of Q with different $(k_0 a_s)^{-1}$ according to Eq.(5). The inset shows ξ_Q in the region near Q_1 . (c) The threshold energy $E_{th}^Q = \min\{E_{th,-}^Q, E_{th,+}^Q\}$. $E_{th,+}^Q$ ($E_{th,-}^Q$) is the threshold energy of a particle A in the upper (lower) helicity branch and a particle B with a c.m. momentum Q . (d) The two-body energy with different interacting strengths by exactly solving Eq. (2). The inset shows the variation of the ground state c.m. momentum. Here $Q_0 = -2k_0 e_x$.

ual meta-stable state, the associated c.m. momentum exhibits similar behavior as in (i). An interesting question then concerns how the system transits among multiple meta-stable states when the interaction is tuned. To address it, suppose for simplicity that E_{th}^Q has two degenerate local minima, respectively at Q_1 and Q_2 and E_Q^{sc} varies monotonically with Q for fixed scattering length. The ground state c.m. momentum Q is expected to be close to Q_1 or Q_2 , depending on which corresponds to a smaller E_Q^{sc} . If the behavior of E_Q^{sc} can be changed by tuning a_s^{-1} , say from increase to decrease with Q , a transition of the system between the two meta-stable states can be induced. This phenomenon also occurs when the two local minima E_{th}^Q become non-degenerate, due to the competition between E_{th}^Q and E_Q^{sc} , as discussed in Ref. [30]. In addition, with the increasing of a_s^{-1} , E_Q^{sc} will dominate over E_{th}^Q in determining the dispersion E_Q . This may qualitative change the dispersion of two-body energy, say from a double-well type to a single-well type.

Spin-orbit coupled three-component Fermi mixture. To corroborate above predictions, below we present concrete calculations by solving Eq. (2) for a system of interacting Fermi mixture of ^{40}K - ^{40}K - ^6Li (A-A-B), where the atom ^{40}K has an equal weight combination of Rashba-type and Dresselhaus-type SOC and the atom ^6Li is spinless, as can be readily realized with the state of the art techniques using cold atoms [19, 32]. The Hamiltonian for

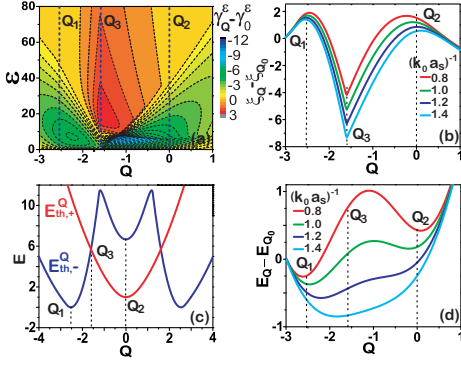


Figure 3. (a) The distribution of $\gamma_Q^\varepsilon - \gamma_0^\varepsilon$. (b) ξ_Q as a function of Q with different $(k_0 a_s)^{-1}$ according to Eq.(5). The inset shows ξ_Q in the region near Q_1 . (c) The threshold energy $E_{th}^Q = \min\{E_{th,-}^Q, E_{th,+}^Q\}$. $E_{th,+}^Q$ ($E_{th,-}^Q$) is the threshold energy of a particle A in the upper (lower) helicity branch and a particle B with a c.m. momentum Q . (d) The two-body energy with different interacting strengths by exactly solving Eq. (2). The inset shows the variation of the ground state c.m. momentum. Here $Q_0 = -3k_0 e_x$.

the system reads

$$H = \sum_{\mathbf{k}, \sigma} \varepsilon_{\mathbf{k}}^a a_{\mathbf{k}, \sigma}^\dagger a_{\mathbf{k}, \sigma} + \sum_{\mathbf{k}} (h a_{\mathbf{k}, \uparrow}^\dagger a_{\mathbf{k}, \downarrow} + \alpha_0 k_x a_{\mathbf{k}, \uparrow}^\dagger a_{\mathbf{k}, \uparrow} + h.c.) + \sum_{\mathbf{k}} \varepsilon_{\mathbf{k}}^b b_{\mathbf{k}}^\dagger b_{\mathbf{k}} + \frac{U}{V} \sum_{\mathbf{k}, \mathbf{k}', \mathbf{q}} a_{\frac{\mathbf{q}}{2} + \mathbf{k}, \uparrow}^\dagger b_{\frac{\mathbf{q}}{2} - \mathbf{k}}^\dagger b_{\frac{\mathbf{q}}{2} - \mathbf{k}'} a_{\frac{\mathbf{q}}{2} + \mathbf{k}', \uparrow}. \quad (6)$$

Here $a_{\mathbf{k}, \sigma}$ ($\sigma = \uparrow, \downarrow$) denotes the annihilation operator of a SOC-free particle A with spin σ and momenta \mathbf{k} , while the operator $b_{\mathbf{k}}$ annihilates a particle B with momenta \mathbf{k} . In addition, $\varepsilon_{\mathbf{k}}^{a(b)} = k^2/(2m_{a(b)})$ is the kinetic energy of particle A(B); α_0 and h respectively parameterize SOC strength and the Zeeman field along \hat{z} direction. Under SOC, the single-particle eigenstates of A in the helicity basis are created by operators $a_{\mathbf{k}, \pm}^\dagger = \lambda_{\mathbf{k}}^{\pm, \uparrow} a_{\mathbf{k}, \uparrow}^\dagger + \lambda_{\mathbf{k}}^{\pm, \downarrow} a_{\mathbf{k}, \downarrow}^\dagger$, with $\lambda_{\mathbf{k}}^{\pm, \uparrow} = \pm \zeta_{\mathbf{k}}^\pm$, $\lambda_{\mathbf{k}}^{\pm, \downarrow} = \zeta_{\mathbf{k}}^\mp$, and $\zeta_{\mathbf{k}}^\pm = [\sqrt{h^2 + \alpha_0^2 k_x^2} \pm \alpha_0 k_x]^{1/2} / \sqrt{2} [h^2 + \alpha_0^2 k_x^2]^{1/4}$, with $+$ ($-$) labelling the upper (lower) helicity branch. The single particle dispersion of the helicity branch are $\varepsilon_{\mathbf{k}, \pm}^a = \varepsilon_{\mathbf{k}}^a \pm \sqrt{h^2 + \alpha_0^2 k_x^2}$. Here we have measured the energy in the unit of $E_0 = 2\alpha^2 m_a / \hbar^2$, the momentum in the unit of $k_0 = 2\alpha m_a / \hbar^2$, and the Zeeman field $h = 0.4E_0$.

We first present our results for the pairing of fermions in the vacuum, as summarized in Fig. 1. The density of states [see Fig. 1(a)] exhibits a monotonic decrease with both Q and the energy ε . As expected, E_Q^{sc} will change monotonically with respect to both Q and a_s^{-1} [see Fig. 1(b)]. Together with E_{th}^Q [see Fig. 1(c)], we see that the actual ground state c.m. momenta will be pulled to the direction with a smaller magnitude than Q_1 and the increase of a_s^{-1} will enhance this tendency [see Fig. 1(d)].

We now turn to the pairing on top of a filled Fermi

sea with the Fermi energy $E_h = -1.5E_0$, as illustrated in Fig. 2. There, both the density of states [see Fig. 2(a)] and E_Q^{sc} [see Fig. 2(b)] exhibit a rich behavior. In addition, from E_{th}^Q in Fig. 2(c), we see that there exist two meta-stable states near Q_1 and Q_2 , respectively. Let us first analyze the c.m. momenta associated with the meta-stable state, e.g., the one formed near Q_1 . Seen from Fig. 2(a), γ_Q^ε for c.m. momentum near Q_1 decreases with Q in the low energy region (e.g. $0 < \varepsilon < 2E_0$), but increases in the high energy region (e.g. $6E_0 < \varepsilon < 10E_0$). In addition, near Q_1 , E_{sc}^Q [see the inset of Fig. 2(b)] shows a qualitative change with increasing of a_s^{-1} . We thus expect from earlier discussions a zigzag behavior of c.m. momenta of the meta-stable state, as confirmed by our results plotted in the inset of Fig. 2(d). Next, we discuss which of the two meta-stable states the system chooses in the ground state. Due to the degeneracy of the two local minima of E_{th}^Q , this is determined by the density of states, which is larger near Q_1 than that near Q_2 [see Fig. 2(a)]. Hence the meta-stable state near Q_1 is energetically favored by E_{sc}^Q [see Fig. 2(b)]. We thus expect the ground state c.m. momentum to be near Q_1 , well agreeing with Fig. 2(d).

Comparing the pairing in the vacuum and on top of the filled Fermi sea, we observe that the presence of Fermi sea not only elevates E_{th}^Q in the regime $Q_1 < Q < Q_2$, giving rise to two minima, but also enhances the density of states there. Consequently, the minimum of E_{sc}^Q occurs at Q_3 , and the two meta-stable states merge together [see Fig. 2(d)] following from previous analysis. We remark that, while the SOC here has dramatically modified the density of states compared to the SOC-free case, our analysis based on perturbation treatment agree remarkably well with the exact numerical results.

Concluding discussions. When the Fermi sea has only one Fermi surface, the two meta-stable states formed near Q_1 and Q_2 are favored by the threshold energy and the density of states, respectively, see Fig. 3. In Ref. [30] with high Fermi energy, tuning the interaction can induce a transition between the two meta-stable states. In contrast, as illustrated in Fig. 3 where the Fermi energy $E_h = 0$, such transition is missing and the increase of a_s^{-1} will eventually cause a merge of the two meta-stable states. With an increase of the Fermi energy, our case crossovers to that discussed in Ref. [30].

Summarizing, we have investigated how the tuning of interacting strength of a repulsive s-wave interaction affect two-body energy under certain distribution of the density of states. Combining with the dispersion of the threshold energy, we can predict typical behavior of the system when tuning the scattering length and hence the interaction, including the change of the c.m. momentum of the ground state and the competition between multiple meta-stable states. Our perturbation analysis is corroborated by the exact numerical solution of the two-body

problem for a spin-orbit coupled Fermi mixture of ^{40}K - ^{40}K - ^6Li , even though the density of states is significantly altered by the effect of SOC.

Acknowledgments We thanks Ying Hu for helpful discussion. The work is supported by the NFRP (Grants No. 2013CBA01502 and No. 2013CB834100), the NNSF of China (Grants No. 11374040, No. 11475027, No. 11575027, No. 11274051 and No. 11547046).

* lbfu@ipacm.ac.cn

- [1] C. Zhang, S. Tewari, R. M. Lutchyn, and S. Das Sarma, Phys. Rev. Lett. **101**, 160401 (2008).
- [2] M. Sato, Y. Takahashi, and S. Fujimoto, Phys. Rev. Lett. **103**, 020401 (2009).
- [3] M. Gong, S. Tewari, and C. Zhang, Phys. Rev. Lett. **107**, 195303 (2011).
- [4] M. Iskin and A. L. Subasi, Phys. Rev. Lett. **107**, 050402 (2011).
- [5] W. Yi and G.-C. Guo, Phys. Rev. A **84**, 031608(R) (2011).
- [6] L. Dell'Anna, G. Mazzaella, and L. Salasnich, Phys. Rev. A **84**, 033633 (2011).
- [7] M. Gong, G. Chen, S. Jia, and C. Zhang, Phys. Rev. Lett. **109**, 105302 (2012).
- [8] L. Han and C. A. R. Sá de Melo, Phys. Rev. A **85**, 011606(R) (2012).
- [9] R. Liao, Y. Yi-Xiang, and W.-M. Liu, Phys. Rev. Lett. **108**, 080406 (2012).
- [10] L. He and X.-G. Huang, Phys. Rev. Lett. **108**, 145302 (2012).
- [11] J. Zhou, W. Zhang, W. Yi, Phys. Rev. A **84**, 063603 (2011).
- [12] X. Yang and S. Wan, Phys. Rev. A **85**, 023633 (2012).
- [13] L. Dong, L. Jiang, and H. Pu, New J. Phys. **15**, 075014 (2013).
- [14] X.-F. Zhou, G.-C. Guo, W. Zhang, and W. Yi, Phys. Rev. A **87**, 063606 (2013).
- [15] X.-J. Liu, K. T. Law, and T. K. Ng, Phys. Rev. Lett. **112**, 086401 (2014).
- [16] Jean Dalibard, Fabrice Gerbier, Gediminas Juzeliūnas, and Patrik Öhberg, Rev. Mod. Phys. **83**, 1523 (2011).
- [17] Zhi-Fang Xu, Li You, and Masahito Ueda, Phys. Rev. A **87**, 063634 (2013); K. Jiménez-García, L. J. LeBlanc, R. A. Williams, M. C. Beeler, C. Qu, M. Gong, C. Zhang, and I. B. Spielman, Phys. Rev. Lett. **114**, 125301 (2015).
- [18] Y.-J. Lin, K. Jiménez-García, and I. B. Spielman, Nature (London) **471**, 83 (2011); J.-Y. Zhang, S.-C. Ji, S. Chen, L. Zhang, Z.-D. Du, J.-W. Pan, Y. Deng, H. Zhai, and Z. Chen, Phys. Rev. Lett. **109**, 115301 (2012).
- [19] P. Wang, Z.-Q. Yu, Z. Fu, J. Miao, L. Huang, S. Chai, H. Zhai, and J. Zhang, Phys. Rev. Lett. **109**, 095301 (2012); L. W. Cheuk, A. T. Sommer, Z. Hadzibabic, T. Yefsah, W. S. Bakr, and M. W. Zwierlein, Phys. Rev. Lett. **109**, 095302 (2012); Lianghai Huang, Zengming Meng, Pengjun Wang, Peng Peng, Shao-Liang Zhang, Liangchao Chen, Donghao Li, Qi Zhou and Jing Zhang, Nat. Phys. **10**, 1038 (2016).
- [20] Cooper L N. Phys Rev, **104**, 1189 (1956); Bardeen J, Cooper L N, Schrieffer J R. Phys Rev, **103**, 1175 (1957).
- [21] Peter Fulde and Richard A. Ferrell, Phys. Rev. **135**, A550 (1964); A.I. Larkin and Y.N. Ovchinnikov, Sov. Phys. JETP **20**, 762 (1965).
- [22] W. Ketterle and M. W. Zwierlein, Rivista del Nuovo Cimento **31**, 247-422 (2008).
- [23] J P. Vyasanakere and V. B. Shenoy, Phys. Rev. B **83**, 094515 (2011).
- [24] J. P. Vyasanakere, S. Zhang, and V. B. Shenoy, Phys. Rev. B **84**, 014512 (2011).
- [25] H. Hu, L. Jiang, X.-J. Liu, and H. Pu, Phys. Rev. Lett. **107**, 195304 (2011).
- [26] Z.-Q. Yu and H. Zhai, Phys. Rev. Lett. **107**, 195305 (2011).
- [27] Ren Zhang, Fan Wu, Jun-Rong Tang, Guang-Can Guo, Wei Yi, and Wei Zhang, Phys. Rev. A **87**, 033629 (2013).
- [28] Vijay B. Shenoy, Phys. Rev. A **88**, 033609 (2013).
- [29] Fan Wu, Ren Zhang, Tian-Shu Deng, Wei Zhang, Wei Yi, and Guang-Can Guo, Phys. Rev. A **89**, 063610 (2014).
- [30] Lihong Zhou, Xiaoling Cui, and Wei Yi, Phys. Rev. Lett. **112**, 195301 (2014).
- [31] C. Chin, R. Grimm, P. Julienne, and E. Tiesinga, Rev. Mod. Phys. **82**, 1225 (2010).
- [32] A. Schirotzek, C.-H. Wu, A. Sommer, and M. W. Zwierlein, Phys. Rev. Lett. **102**, 230402 (2009); M. Koschorreck, D. Pertot, E. Vogt, B. Fröhlich, M. Feld, and M. Köhl, Nature (London) **485**, 619 (2012).
- [33] We note that for homo-nuclear systems, our derivation for $\gamma_{\mathbf{Q}}^{\epsilon}$ reduces to the singlet density of states as discussed in Ref. [28].
- [34] With Eq.(3) and renormalization equation, we have $\int_0^{\infty} \frac{\gamma_0^{\epsilon} d\epsilon}{\epsilon_b - \epsilon} d\epsilon = \int_0^{\infty} \frac{\gamma_{\mathbf{Q}}^{\epsilon}}{\xi_{\mathbf{Q}} + \epsilon_b - \epsilon} d\epsilon$. The right hand of the equation can be written as follow $\int_0^{\infty} \frac{\gamma_{\mathbf{Q}}^{\epsilon}}{\xi_{\mathbf{Q}} + \epsilon_b - \epsilon} d\epsilon = \int_0^{\infty} [\frac{\gamma_{\mathbf{Q}}^{\epsilon}}{\epsilon_b - \epsilon} - \frac{\xi_{\mathbf{Q}} \gamma_{\mathbf{Q}}^{\epsilon}}{(\epsilon_b - \epsilon)^2} + \frac{2\xi_{\mathbf{Q}}^2 \gamma_{\mathbf{Q}}^{\epsilon}}{(\epsilon_b - \epsilon)^3} + \dots] d\epsilon$. To first order of $\xi_{\mathbf{Q}}$ ($|\frac{\xi_{\mathbf{Q}}}{\epsilon_b}| \ll 1$), we arrive Eq.(5).
- [35] Xiaoling Cui, Phys Rev A **85**, 022705 (2012).
- [36] P. Zhang, L. Zhang, and Y. Deng, Phys. Rev. A **86**, 053608 (2012).
- [37] P. Zhang, L. Zhang, and W. Zhang, Phys. Rev. A **86**, 042707 (2012).
- [38] Y. Wu and Z. Yu, Phys. Rev. A, **87**, 032703 (2013).
- [39] Hao Duan, Li You, and Bo Gao, Phys. Rev. A, **87**, 052708 (2013).
- [40] $\frac{\partial \xi_{\mathbf{Q}}}{\partial a_s^{-1}} = \frac{a_s^{-1}}{m_{\mu}} \int_0^{\infty} f_{\epsilon} (\gamma_{\mathbf{Q}}^{\epsilon} - \gamma_0^{\epsilon}) d\epsilon$ with $f_{\epsilon} = \int_0^{\epsilon} \frac{\gamma_{\mathbf{Q}}^{\epsilon'} (\epsilon - \epsilon')^2}{(\epsilon - \epsilon_b)^3 (\epsilon' - \epsilon_b)^3} d\epsilon' > 0$. Using the mean value theorem of integrals, we have $\frac{\partial \xi_{\mathbf{Q}}}{\partial a_s^{-1}} = f_{\epsilon_c} \frac{a_s^{-1}}{m_{\mu}} \int_0^{\infty} (\gamma_{\mathbf{Q}}^{\epsilon} - \gamma_0^{\epsilon}) d\epsilon$.
- [41] the analysis for the case with $\gamma_{\mathbf{Q}}^{\epsilon} - \gamma_0^{\epsilon} > 0$ is similar.